Chinese Journal of Polymer Science Vol. 34, No. 6, (2016), 739−754

Chinese Journal of Polymer Science

Investigation of Structural, Rheological and Thermal Properties of PMMA/ONi-Al LDH Nanocomposites Synthesized *via* Solvent Blending Method: Effect of LDH Loading

Samarshi Chakraborty, Manish Kumar, Kelothu Suresh and G. Pugazhenthi*
Department of Chemical Engineering, Indian Institute of Technology Guwahati, Guwahati 781039, India

Abstract This article addresses the synthesis of organically tailored Ni-Al layered double hydroxide (ONi-Al LDH) and its use in the fabrication of exfoliated poly(methyl methacrylate) (PMMA) nanocomposites. The pristine Ni-Al LDH was initially synthesized by co-precipitation method and subsequently modified using sodium dodecyl sulfate to obtain ONi-Al LDH. Nanocomposites of PMMA containing various amounts of modified Ni-Al LDH (3 wt%–7 wt%) were synthesized *via* solvent blending method to investigate the influence of LDH content on the properties of PMMA matrix. Several characterization methods such as X-ray diffraction (XRD), transmission electron microscopy (TEM), Fourier transform infrared spectroscopy (FTIR), rheological analysis, differential scanning calorimetry (DSC) and thermo gravimetric analysis (TGA), were employed to examine the structural, viscoelastic and thermal properties of PMMA/OLDH nanocomposites. The results of XRD and TEM examination confirm the formation of partially exfoliated PMMA/OLDH nanocomposites. The FTIR results elucidate that the characteristic bands for both pure PMMA and modified LDH are present in the spectra of PMMA/OLDH nanocomposites. Rheological analyses were carried out to examine the adhesion between polymer matrix and fillers present in the nanocomposite sample. The TGA data indicate that the PMMA nanocomposites exhibit higher thermal stability when compared to pure PMMA. The thermal decomposition temperature of PMMA/OLDH nanocomposites increases by 28 K compared to that of pure PMMA at 15% weight loss as a point of reference. In comparison with pure PMMA, the PMMA nanocomposite containing 7 wt% LDH demonstrates improved glass transition temperature (T_g) of around 3 K. The activation energy (E_a), reaction orders (n) and reaction mechanism of thermal degradation of PMMA/OLDH nanocomposites were evaluated using different kinetic models. Water uptake capacity of the PMMA/OLDH nanocomposites is less than that of the pure PMMA.

Keywords: Ni-Al LDH; PMMA; XRD; FTIR; TGA; Kinetic model.

INTRODUCTION

Polymer nanocomposite (PNC) was first invented in Toyota Central R & D labs, in 1985[1]. The new concept of polymer nanocomposite expanded the fields of polymer science and led to new applications for automotive, electric and food packaging industries. Polymer/clay nanocomposites are a new kind of composites in which inorganic nanoparticles are inserted as additives inside the polymer matrix to improve the properties, including structural, mechanical, thermal properties[2–4], gas barrier effect[5, 6] and fire retardancy[7, 8] compared to pure polymers. Nanoparticles incorporation into the polymer matrix helps to enhance the properties of polymer only when the nanoparticles are well dispersed in the polymer matrix. Three types of nanocomposite structure can be observed when the nanoparticles are dispersed into the polymer matrix, which include immiscible, intercalated and exfoliated nanocomposites[9]. It is generally considered that exfoliated nanocomposites structure is the most desirable for improving nanocomposite properties, for example mechanical properties, but it is not a necessity

* Corresponding author: G. Pugazhenthi, E-mail: pugal@iitg.ernet.in
Received December 16, 2015; Revised January 19, 2016; Accepted January 24, 2016
doi: 10.1007/s10118-016-1786-4

for improving flammability properties.

There are mainly four ways to prepare polymer nanocomposites, discussed in the literature, including melt compounding[10, 11], *in situ* polymerization[12, 13], emulsion/suspension polymerization[14] and solvent blending[15–18]. Amongst these, solvent blending method consistently gives intercalated or exfoliated nanocomposites depending on the polymer and clay compatibility. A series of literatures demonstrated the fabrication of PMMA/MMT nanocomposites using various techniques[7, 15]. Huskic *et al.*[15] synthesized PMMA/MMT nanocomposites by solution polymerization technique and the prepared nanocomposites exhibited an enhanced glass transition temperature (T_g) of 4–9 K over that of the neat PMMA. They also reported that an increased solvent resistance of the nanocomposite was due to the hindered path of the solvent molecules through the polymer matrix. Wang *et al.*[7] reported that the nanofiller, such as kaolinite, LDH and MMT, had greatly influenced the thermal properties of PMMA nanocomposites. Thermal stability of the nanocomposite was improved by about 10, 21 and 29 K over that of the neat PMMA by the addition of kaolinite, LDH and MMT, respectively. The influence of organoclay loading on the thermal, mechanical and fire retardancy properties of PMMA/clay nanocomposites was investigated by Unnikrishnan and coworkers[19] and the thermal degradation kinetics of the prepared nanocomposites was also examined using Kissinger and Flynn-Wall-Ozawa models.

Majority of the PMMA nanocomposites were prepared using cationic clays, like MMT (montmorillonite), whereas LDHs are less examined due to their strong electrostatic interaction, small gallery space and hydrophilic nature. This problem can be resolved with modification of LDHs using surfactants. Thanks to highly tunable properties of LDH, it is considered as the most preferable layered crystal for preparing multifunctional polymer/layered crystal nanocomposites[20]. LDHs are layered crystalline materials containing anionic counter ions in the gallery space. It is represented by the general chemical formula: $[M^{2+}_{1-x}\, M^{3+}_{x}(OH)_2]^{x+}(A^{m-})_{x/m}\, yH_2O$, where, M^{2+} is a divalent cations (such as Ni^{2+}, Mg^{2+}, Cu^{2+}), M^{3+} is a trivalent cation (such as Al^{3+}, Cr^{3+}) , A is an interlayer anion with *m*- charge, and *y* is a fraction constant[21]. The Ni-Al LDH can be easily synthesized in the laboratory with high purity and tunable chemical compositions. The Ni-Al LDH exhibits potential advantages in flame retardants[22], medical field[23] and capacitors[24, 25] .

In recent years, numerous researchers have been working on polymer/LDH nanocomposites. They have adopted various preparation methods and studied structural and thermal properties, including thermal degradation kinetics of the prepared polymer nanocomposites[12, 14, 16, 17]. Qu *et al.*[14] prepared exfoliated polystyrene (PS)/Mg-Al LDH nanocomposites using emulsion polymerization. They reported about 19 K improvement in thermal stability of a PS/LDH 5 (5 wt% LDH loading) nanocomposite compared to pure PS, when 50% weight loss was considered as reference point. In our prior work[16], we have achieved the formation of exfoliated PS/Co-Al LDH nanocomposites with 5 wt% LDH loading. In comparison with pure PS, thermal decomposition temperature of PS nanocomposites with 5 wt% LDH was enhanced by 12 K. Several researchers have been working on PMMA/LDH nanocomposites due to their enormous potential in various fields of application. Wang *et al.*[13] prepared disorderly exfoliated LDHs/PMMA nanocomposites using *in situ* bulk polymerization of MMA in presence of various LDH-U contents. The glass transition temperature (T_g) was 22 K higher for exfoliated PMMA/LDHs nanocomposites than that of pure PMMA. The improved thermal and flammability properties of PMMA/LDH nanocomposites were clearly demonstrated by several other researchers[26–28]. Chen *et al.*[29] reported that the incorporation of Zn-Al LDH into the poly(methyl-acrylate) matrix enhanced the mechanical properties, the tensile strength of the PMA/Zn-Al LDH nanocomposite increased to 3.81 MPa, much higher than that of the pure PMA (0.46 MPa).

The rheological study of polymer nanocomposites is another key aspect of investigation for researchers working on PNC. Zhou *et al.*[30] synthesized PMMA/carbon nanotube (CNT) nanocomposites by emulsion method and reported that modified CNT's have higher percolation in comparison with unmodified CNT's. Ivanov *et al.*[31] studied two different grades of polypropylene (MM1 and MA3) and reported that dynamic viscosity of MA3/hydrogenated oligo cyclopentadiene (EP1) blends decreased with increasing EP1 modifier concentration. In another study[32], it was found that the complex viscosity and storage modulus increased as the carbon nanofiber concentration increased in the ethylene propylene copolymer matrix.

With respect to the prior work reviewed above and to best of our knowledge, there is no work reported on the synthesis of PMMA/Ni-Al LDH nanocomposites till date. In view of this, the fabrication of PMMA/Ni-Al LDH nanocomposites *via* solvent blending method and influence of LDH loading on structural, rheological and thermal properties of the PMMA matrix are explored in this work.

EXPERIMENTAL

Raw Material

Poly(methyl methacrylate) was purchased from LG Polymer, South Korea. Nickel nitrate ($Ni(NO_3)_2 \cdot 6H_2O$), aluminum nitrate ($Al(NO_3)_3 \cdot 9H_2O$), sodium nitrate ($NaNO_3$), sodium hydroxide (NaOH), methylene chloride (CH_2Cl_2), sodium dodecyl sulfate ($NaC_{12}H_{25}SO_4$) were purchased from Merck, India. Millipore water was used throughout the experiment.

Synthesis and Modification of Ni-Al LDH

Ni-Al LDH was synthesized by the co-precipitation method. For this, an aqueous solution of $Ni(NO_3)_2 \cdot 6H_2O$, $Al(NO_3)_3 \cdot 9H_2O$ and $NaNO_3$ was firstly prepared using the mole ratio of the nitrate salts as 2:1:2, respectively. Then, NaOH solution (2 mol/L) was added drop wise into the above solution with continuous stirring until the pH level reached 10 and the resulting solution was stirred for 16 h at room temperature. The obtained final solution was filtered and the precipitate was washed with Millipore water until neutral. Then the precipitate was dried at room temperature for 24 h and at 65 °C for 6 h in an oven. For the modification of LDH, 2.5 g of dried pristine LDH was calcined at 500 °C for 5 h in muffle furnace. After calcination, the LDH was modified with sodium dodecyl sulfate (SDS) for better dispersion of LDH in the polymer matrix. The calcined LDH was dispersed into 120 mL of aqueous solution containing 2.5 g of SDS and refluxed at 80 °C for 12 h to yield modified LDH. Finally it was filtered and dried at 50 °C in an oven. Then the modified Ni-Al LDH sample was grinded into finer particles.

Preparation of PMMA/ONi-Al LDH Nanocomposites

A small amount of nanofiller addition into the polymer matrix enhances the properties of the nanocomposites and hence, the study of effects of LDH content on the properties of PMMA nanocomposites is essential. PMMA/OLDH nanocomposites were prepared with 3 wt%, 5 wt% and 7 wt% of OLDH loading (relative to PMMA) by solvent blending method using methylene chloride as a solvent. Before synthesis of nanocomposites, both PMMA and organomodified Ni-Al LDH (OLDH) were dried in an oven at 80 °C and 70 °C, respectively for 12 h to remove moisture. After that, a desired quantity of ONi-Al LDH was dispersed in 30 mL of methylene chloride and stirred for 24 h at room temperature (25 °C) and then sonicated (Sonics and Materials, Model VCX 500) for 30 min (referred as solution-A). LDH dispersion was checked after 24 h by keeping the solution A undisturbed for 1 h. If any settling of LDH was noticed, the sample was sonicated again. A calculated amount of PMMA was mixed with 42 mL of methylene chloride and stirred at room temperature till the PMMA completely dissolved (solution-B). Then these above prepared two solutions (solutions A and B) were mixed and stirred for 12 h at room temperature. The schematic diagram for preparation of PMMA/Ni-Al LDH nanocomposites is represented in Fig. 1. The resulting PMMA/OLDH solution was spread over a Petri dish and left for 24 h in ambient condition yielding a viscous gel layer. Finally, the nanocomposite films were dried in an oven at 65 °C for 6 h. Hereafter, PMMA nanocomposites prepared using 3 wt%, 5 wt% and 7 wt% of OLDH were referred as PMMA/OLDH 3, PMMA/OLDH 5 and PMMA/OLDH 7, respectively. For comparison purpose, the blank PMMA film was also synthesized by an identical procedure in the absence of LDH. All the experiments/analyses were conducted in duplicate and the average values were reported.

Characterization and Measurements

X-ray diffraction (XRD) measurements were performed for LDH and PMMA nanocomposite samples at room temperature using an AXS D8 ADVANCE Powder X-ray Diffractometer (Bruker) equipped with Ni-filtered Cu Kα radiation (λ = 0.15418 nm). The patterns were acquired over a 2θ range of 2°−50° with an increment of

0.05° and scan speed of 0.5 sec. The basal spacing distance of LDH layer was calculated from the estimation of (003) plane peak using the Bragg equation: $\lambda = 2d\sin\theta$, where λ is the wavelength (λ = 0.15418 nm). TEM observations were carried out on a JEOL JEM-2100 microscope with an accelerating voltage of 200 kV to identify the structure of polymer nanocomposites. The FTIR spectra of LDH and PMMA nanocomposites were recorded using a Perkin Elmer Fourier transform infrared spectroscope. The surface morphology was analysed using an atomic force microscope (AFM), Model No. 5500 series, Agilent Technologies, USA in non-contact mode. The scan angle was perpendicular to the surface of specimen. All offline image flattening and analyses of the images were conducted using a software, WSxM v5.0. The thermo-gravimetric analyses were performed under nitrogen atmosphere on a TGA/SDTA851e/LF/1100 model (Mettler Toledo, Greifensee, Switzerland) instrument in the temperature range of 25 to 700 °C with a heating rate of 10 K/min. A Mettler Toledo-1 series differential scanning calorimeter (DSC) was employed to examine the glass transition temperature of the PMMA nanocomposites. Samples were heated from 25 °C to 200 °C at a heating rate of 5 K/min under nitrogen atmosphere. The rheological properties of pure PMMA and PMMA/OLDH nanocomposites were measured by using an Anton Paar MCR 301 rheometer in an oscillation mode with parallel plate geometry using 50 mm diameter disc, having thickness of 1 mm at 190 °C.

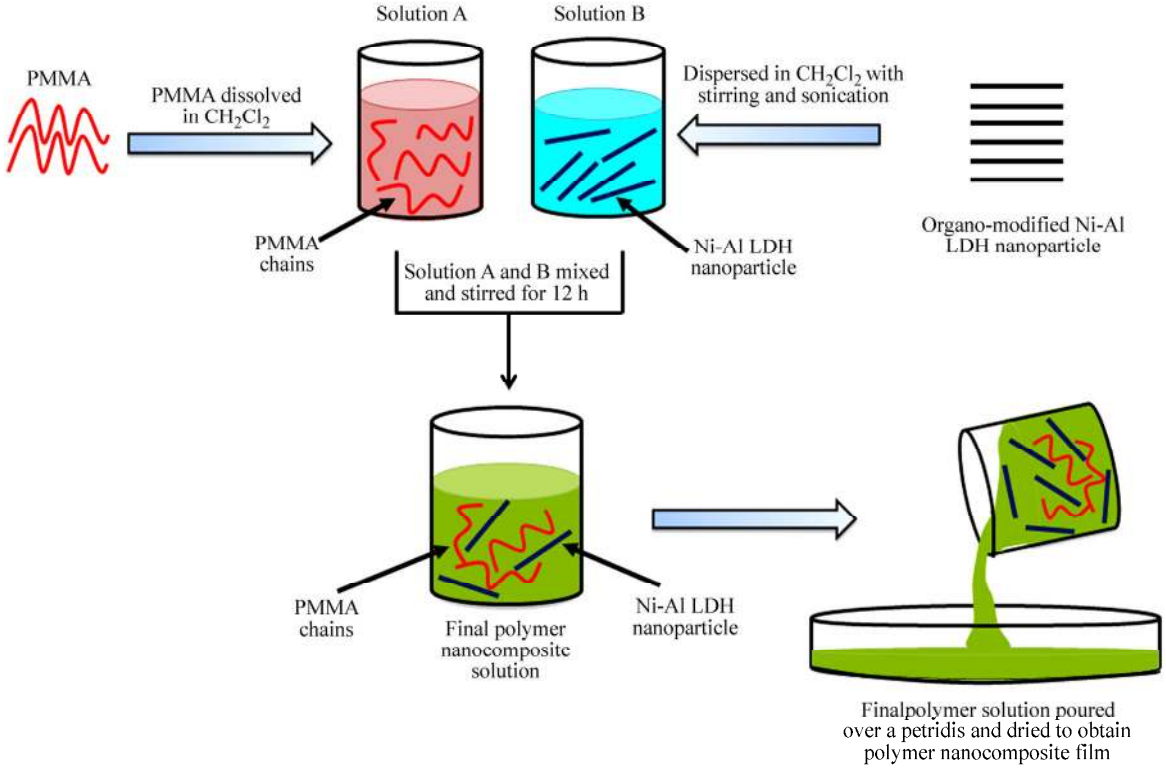

Fig. 1 Schematic diagram for the preparation of PMMA/Ni-Al LDH nanocomposites

Water uptake test is considered as a standard method to measure the water resistance nature of the nanocomposite films. Water uptake capacity of the nanocomposite film was measured by taking weight before and after hydration. The nanocomposite films having dimensions of 2 cm × 2 cm were taken and dried at 80 °C for 4 h to bring all the samples to a similar state. After which, the dry weight (W_d) of the samples was measured. Each of the dried samples was then dipped into individual flasks containing Millipore water for 48 h. Then these samples were taken out, wiped the surface with tissue paper, and weighed immediately. The water uptake capacity of the nanocomposite films was calculated using the following equation.

$$\text{Water uptake (\%)} = \left(\frac{W_w - W_d}{W_d} \right) \times 100$$

where W_w and W_d are the wet and dry weights of nanocomposite films, respectively. Five measurements were performed for each nanocomposite sample and the average value was reported.

RESULTS AND DISCUSSION

XRD Analysis

The XRD analysis is one of the efficient methods to examine the types of a layered structure, whether it is exfoliated or intercalated. This can be observed by changing of peak with the gallery height of the organoclay. Figure 2 demonstrates the XRD patterns of modified Ni-Al LDH and different PMMA nanocomposites. The position of basal peak (003) of LDH indicates the distance between two adjacent metal hydroxide sheets. The basal spacing (d_{003}) of (003) peak for SDS modified LDH at 2θ value of 6.54° is 1.35 nm. The XRD results display that the modified LDH is crystalline in nature and has layered geometry. The obtained results are in accordance with our previous study[17] as well as works reported by other researchers[12, 14]. It appears that the modified basal spacing between interlayers is due to the intercalation of anionic alkyl surfactant. It is well documented that in order to eliminate the stronger electrostatic interaction between LDH layers and achieve intercalated or exfoliated nanocomposite structure, surfactant molecules have been used to modify the LDH's[8, 29].

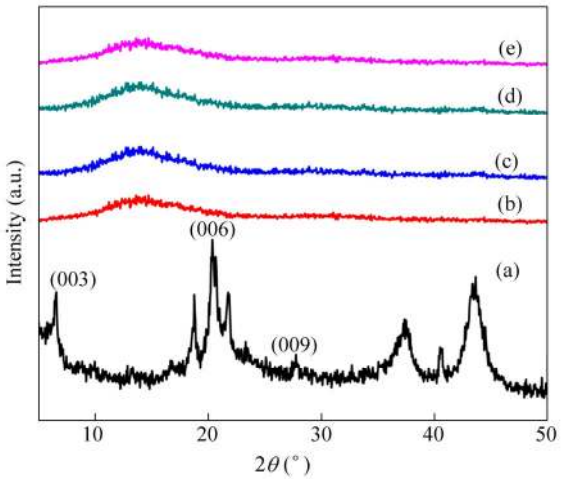

Fig. 2 XRD patterns of (a) modified Ni-Al LDH, (b) pure PMMA, (c) PMMA/OLDH 3, (d) PMMA/OLDH 5 and (e) PMMA/OLDH 7 nanocomposites

In the intercalated nanocomposite structures, the *d*-spacing value generally increases when compared to the LDH, because of the partial penetration of PMMA chains between the LDH layers. In case of exfoliated structure, d_{003} peak will completely disappear due to extensive polymer penetration inside the LDH layer making it disordered. Here in the Fig. 2, the modified LDH possesses (003) peak whereas in the PMMA/OLDH nanocomposites, no (003) peak corresponding to organically modified Ni-Al LDH is seen. In order to study the effect of OLDH loading on the structure of PMMA/OLDH nanocomposites, PMMA/OLDH nanocomposites were prepared with 3 wt%, 5 wt% and 7 wt% LDH loading. Up to 7 wt% LDH loading, no diffraction peak corresponding to (003) is observed. These results are good agreement with other works on polymer/LDH systems[12, 33]. Two extreme cases can explain the disappearnce of the diffaraction peak (003) in XRD: (i) complete exfolation of the layers in the polymer matrix, and/or (2) disordering of the LDH layers within the PMMA matrix or when layer spacing goes beyond 10 nm[34]. It should be noted that even though the XRD

analysis enlightens us the gallery spacing, it is not adequate to depict the dispersion of LDHs in polymer matrix. Hence, TEM analysis needs to be performed to get a qualitative understanding of the internal structure, spatial distribution and dispersion of LDHs through direct visualization. The result of TEM study is discussed in the later section.

FTIR Analysis

In order to ensure that LDH is dispersed in the PMMA matrix, FTIR analysis of PMMA nanocomposites was performed and the obtained results were compared with those of LDH and pure PMMA. FTIR spectra of modified LDH, pure PMMA and PMMA nanocomposites are shown in Fig. 3. For organo-modified Ni-Al LDH, the band in the range of 3400–3500 cm^{-1} is primarily due to O—H stretching vibration of hydrogen-bonded metal hydroxide layer and interlayer water molecules. The characteristic stretching band for aliphatic chain ($-CH_2$) of SDS modifier is observed at around 2850–2970 cm^{-1}. The symmetric vibration ($\nu_{S=O}$) of sulfate band exhibits at 1216 cm^{-1}, while the asymmetric vibration ($\nu_{o\ S=O}$) appears between 1050–1100 cm^{-1}. Both peaks are related to modification of LDH by sodium dodecyl sulfate (SDS). The bands recorded at the low frequency region of 400–800 cm^{-1} correspond to the vibration of the metal-oxygen bond in the brucite-like lattice. For PMMA and its nanocomposites, a characteristic peak is observed at 1737 cm^{-1} which represents the >C=O group present in the polymer. The absorbance bands occur in the region of 2700–3000 cm^{-1}, particularly at 2995 and 2949 cm^{-1} is primarily due to C—H stretching vibrations of CH_3 and methylene (CH_2) groups. The remaining PMMA characteristic peaks in the wavenumber ranges of 1490–1437 and 1070 cm^{-1} are assigned to $O-CH_3$ deformation and $O-CH_2$ stretching vibration, respectively[35]. It is observed that the spectra of all nanocomposites have similar peaks with those of pure PMMA, as well as some additional small peaks coming from the ONi-Al LDH (metal-oxygen bonds). From the FTIR analysis, it is proved that the PMMA nanocomposites possess both PMMA and OLDH characteristics.

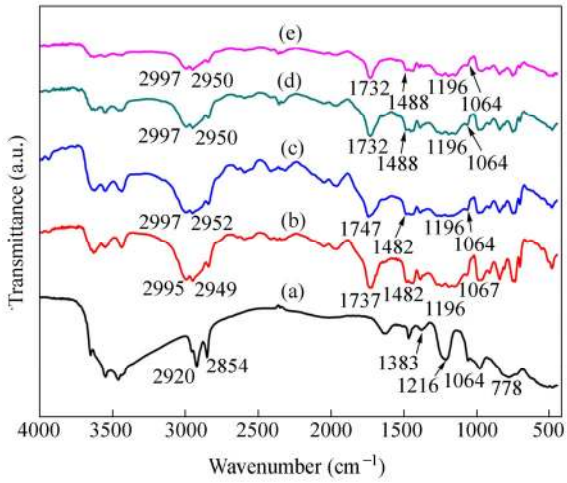

Fig. 3 FTIR spectra of (a) modified LDH, (b) pure PMMA, (c) PMMA/OLDH 3, (d) PMMA/OLDH 5 and (e) PMMA/OLDH 7 nanocomposites

TEM Analysis

The XRD analysis suggests a convenient scheme to determine nanocomposite structure up to 1–4 nm range. When layer spacing goes beyond 10 nm in the intercalated nanocomposite or when the structure becomes disordered, XRD technique is not very useful to analyze the nanocomposite structure. Morgan *et al.*[36] suggests that XRD analysis cannot be considered as a stand-alone technique to analyze nanocomposite structure and additionally, TEM analysis is required to confirm the formation of intercalated or exfoliated nanocomposite structures. TEM analysis is used to correlate the morphological evidence from XRD. Figure 4 depicts the TEM images of PMMA/OLDH 3 and PMMA/OLDH 5 samples. The dark lines denote the LDH layers, whereas the

bright area shows the PMMA matrix. It is observed from Fig. 4(a) that the LDH layers are dispersed in intercalated form in polymer matrix for PMMA/OLDH 3 sample. While the mixed morphology *i.e.* partially intercalated and exfoliated, is exhibited in PMMA/OLDH 5 sample (see Fig. 4b). The 'E' represents the exfoliated structure and 'I' denotes the intercalated state. TEM images clearly demonstrate the formation of partially exfoliated nanocomposites. The obtained results are in good agreement with the works of Wang *et al.*[7] and Nyambo *et al.*[26] on PMMA/LDH nanocomposites.

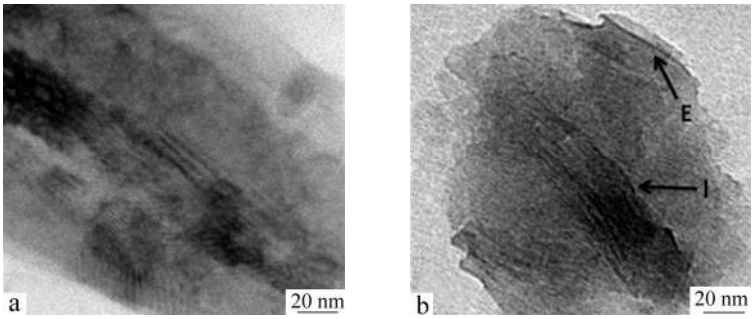

Fig. 4 TEM images of (a) PMMA/OLDH 3 and (b) PMMA/OLDH 5 nanocomposites

AFM Analysis

The AFM analysis of PMMA/OLDH nanocomposite was carried out to access the effect of nanoparticle loading on the surface morphology of the nanocomposite films. The incremental addition of Ni-Al LDH leads to increase the surface roughness of the nanocomposite films. It is clearly seen that pits are present in all the images. The minimum surface roughness is observed for the PMMA/OLDH nanocomposite with 3% loading, whereas maximum roughness is seen in the case of PMMA/OLDH nanocomposite with 7% loading. To confirm measurement repeatability, each nanocomposite (for 3%–7% loading) film is scanned in two separate locations and corresponding values are presented in Table 1. The 3D pictorial representation of each sample is displayed in Figs. 5(a)–5(c).

Table 1. Roughness analysis chart of PMMA/OLDH nanocomposites

Samples	Measurement at two different locations	Surface roughness (nm)
PMMA/OLDH 3	1	12.91
	2	13.03
PMMA/OLDH 5	1	14.85
	2	15.00
PMMA/OLDH 7	1	17.44
	2	17.47

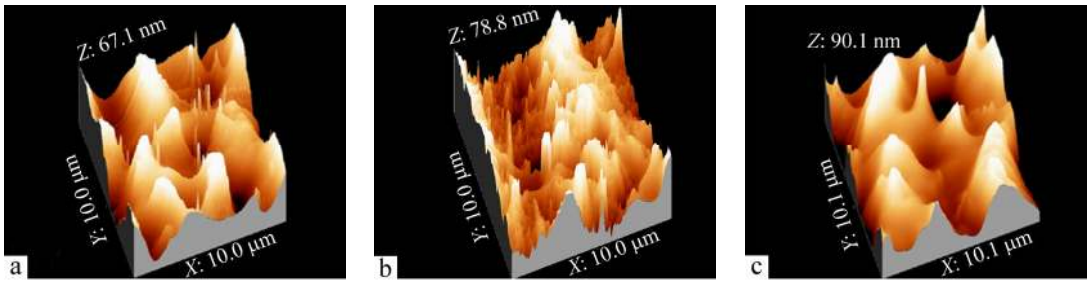

Fig. 5 AFM images of (a) PMMA/OLDH 3, (b) PMMA/OLDH 5 and (c) PMMA/OLDH 7 nanocomposites

TGA Analysis

Thermogravimetric analysis gives us an idea about the thermal stability of the polymer nanocomposites. Figure 6(a) shows TGA curves for ONi-Al LDH, pure PMMA and its nanocomposites with different LDH loadings. The main weight loss of organically modified Ni-Al LDH takes place due to loss of interlayer water molecules, destruction of alkyl chains of the SDS molecule and loss of hydroxide from LDH layers. Taking 15% weight loss as a point of comparison, the thermal decay temperature of ONi-Al LDH is 639 °C. The thermal degradation of pure PMMA mainly occurs in the temperature range of 300–421 °C and no residue is left beyond 430 °C. Generally, PMMA nanocomposites exhibit weight loss in two main steps. The first step of weight loss occurs mainly in the temperature range of 120–250 °C due to the evaporation of physically absorbed water molecules in the interlayer, thermal decompositions of alkyl chains of the SDS molecules and loss of hydroxide from LDH layers. The second step of weight loss starts from 250–440 °C due to thermal degradation of PMMA and the formation of black char. Thermal degradation rate of PMMA nanocomposites is much slower in this step compared to pure PMMA. Slow degradation rate of PMMA nanocomposites is attributed to the hindered effect of LDH layers on diffusion of volatile products throughout the composite material. Above 500 °C, all the curves become flat because only inorganic residues remain at that temperature. Therefore, as a result only pure PMMA exhibits degradation at lower temperature. When 15% weight loss is taken as a point of comparison, the decomposition temperature of pure PMMA, PMMA/OLDH 3, PMMA/OLDH 5 and PMMA/OLDH 7 is 320, 345, 346 and 348 °C, respectively (see Table 2). This clearly shows the improvement of thermal decomposition temperature of PMMA nanocomposites by 25–28 K when compared to pure PMMA. This improvement is due to the strong interaction between PMMA and LDH layers. Wang *et al.*[7] synthesized the Mg-Al LDH by co-precipitation method and exhibited a 15 K enhancement in thermal degradation temperature of PMMA nanocomposites over pure PMMA at 10% weight loss as a reference point. Nyambo *et al.*[26] reported that the thermal decomposition temperature of PMMA/Mg-Al LDH nanocomposites over pure PMMA was improved by 7–19 K when 10% weight loss was selected as the point of comparison. Similar type of results can be observed when 50% weight loss is chosen as a point of comparison. The decomposition temperature of pure PMMA, PMMA/OLDH 3, PMMA/OLDH 5 and PMMA/OLDH 7 is found to be 364.2, 372, 373 and 376 °C respectively. The TGA derivative curves of pure PMMA and its nanocomposites are represented in Fig. 6(B), where the peak indicates a maximum degradation temperature (T_{max}). The T_{max} peaks get shifted to the right hand side for all the PMMA/OLDH nanocomposites compared to pure PMMA. This is indicative of better thermal stability of PMMA nanocomposites when compared to pure PMMA.

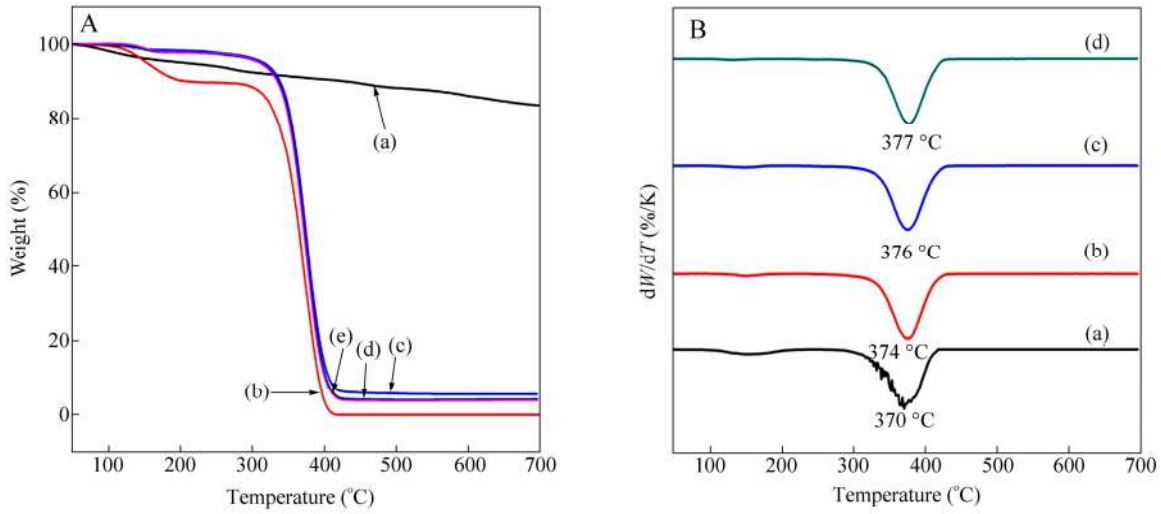

Fig. 6 (A) TGA graphs of (a) Ni-Al LDH, (b) pure PMMA, (c) PMMA/OLDH 3, (d) PMMA/OLDH 5 and (e) PMMA/OLDH 7 nanocomposites; (B) TGA derivatives of (a) pure PMMA, (b) PMMA/OLDH 3, (c) PMMA/OLDH 5 and (d) PMMA/OLDH 7 nanocomposites

Table 2. TGA results of pure PMMA and PMMA/OLDH nanocomposites

Samples	Temperature at 15% weight loss (T_{15}) (°C)	Temperature at 50% weight loss (T_{50}) (°C)	T_{max} (°C)	IPDT (°C)
Pure PMMA	320	364.2	370	351.5
PMMA/OLDH 3	345	372.5	374	399.4
PMMA/OLDH 5	346	373.2	376	406.7
PMMA/OLDH 7	348	376	377	423.6

DSC Analysis

Differential scanning calorimetry (DSC) is used to study the phase transitions like fusion, crystallization and glass transition temperature (T_g). Figure 7 depicts the DSC thermograms of PMMA nanocomposites. The glass transition temperature is determined at the inflection point between the onset and end set temperature. T_g of nanocomposites slightly increases with an increase in the LDH loading. T_g values of pure PMMA, PMMA/OLDH 3, PMMA/OLDH 5 and PMMA/OLDH 7 are 110.5, 112.6, 113 and 114 °C, respectively. It can be seen from the DSC analysis that T_g of PMMA/OLDH 7 is 3 K higher than that of the pure PMMA. Unniskrishnan *et al.*[19] also observed marginal improvements in T_g value (less than 2 K) for PMMA/MMT nanocomposites. In another study, Mohanty and Nayak[37] reported an increase of T_g value of 0.45 K for PMMA/PMMA-MA/B109 nanocomposite over pure PMMA. An increase in the T_g value is due to the restricted movements of PMMA chains, between the LDH interlayer. Even if only one end of the PMMA chain is constrained by the LDH layers, it will still increase the T_g value. According to Shen *et al.*[38] intercalation and exfoliation lead to reduction in polymeric free volume, which is caused by the presence of polymeric chains in the clay interlayer. This concept shows that restricted molecular motion at the PMMA/LDH interface improves the T_g value. Stretz *et al.*[39] explained that T_g of intercalated nanocomposites depends on various factors such as nature of modifier, clay loading, basal spacing and arrangement of clay layers.

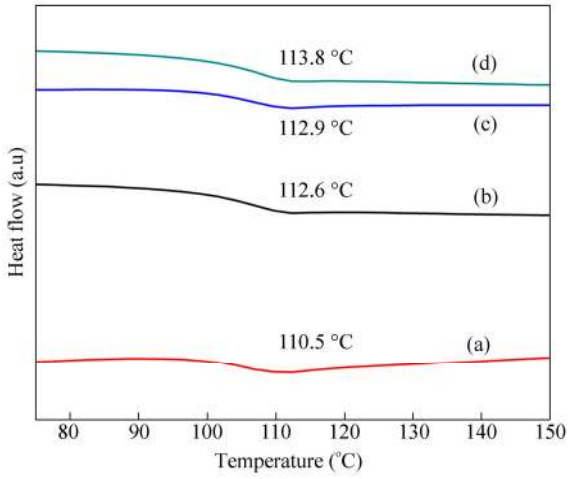

Fig. 7 DSC graphs of (a) pure PMMA, (b) PMMA/OLDH 3, (c) PMMA/OLDH 5 and (d) PMMA/OLDH 7 nanocomposites

Thermal Degradation Kinetic Analysis

Coats-Redfern method

Thermal degradation kinetic parameters, such as the order of reaction (n), pre-exponential factor (A) and apparent activation energy (E_a), were calculated using the Coats-Redfern method[26, 40] as follows:

$n = 1$

$$\ln\left(-\frac{\ln(1-\alpha)}{T^2}\right) = \ln\left[\frac{AR}{\beta E_a}\left(1-\frac{2RT}{E_a}\right)\right] - \frac{E_a}{RT} \tag{1a}$$

$n \neq 1$

$$\ln\left(\frac{1-(1-\alpha)^{1-n}}{(1-n)T^2}\right) = \ln\left[\frac{AR}{\beta E_a}\left(1-\frac{2RT}{E_a}\right)\right] - \frac{E_a}{RT} \tag{1b}$$

where α is the fractional weight loss or conversion degree, β is the heating rate, R is the gas constant and T denotes the temperature.

The Coats-Redfern method requires the TG data with only one heating rate to calculate kinetic parameters. In this study, TGA data of PMMA nanocomposite samples with different LDH loadings were taken at a single heating rate (10 K/min). For this method, a reaction order, n is assumed and the assumed value is substituted in the Eq. (1). The plot of the left hand side of Eq. (1) versus $-1/T$ is fitted linearly, to calculate the correlation coefficient (R^2) and the trial is repeated till the best R^2 value is obtained. Figures 8(a)–8(d) show all the linear fitted graphs of pure PMMA and PMMA/OLDH nanocomposites with different LDH loadings. The calculated reaction order at the best R^2 value is considered as the reaction order for that sample. Then the activation energy and pre-exponential factor are calculated from the slope and intercept of the fitted straight line, respectively.

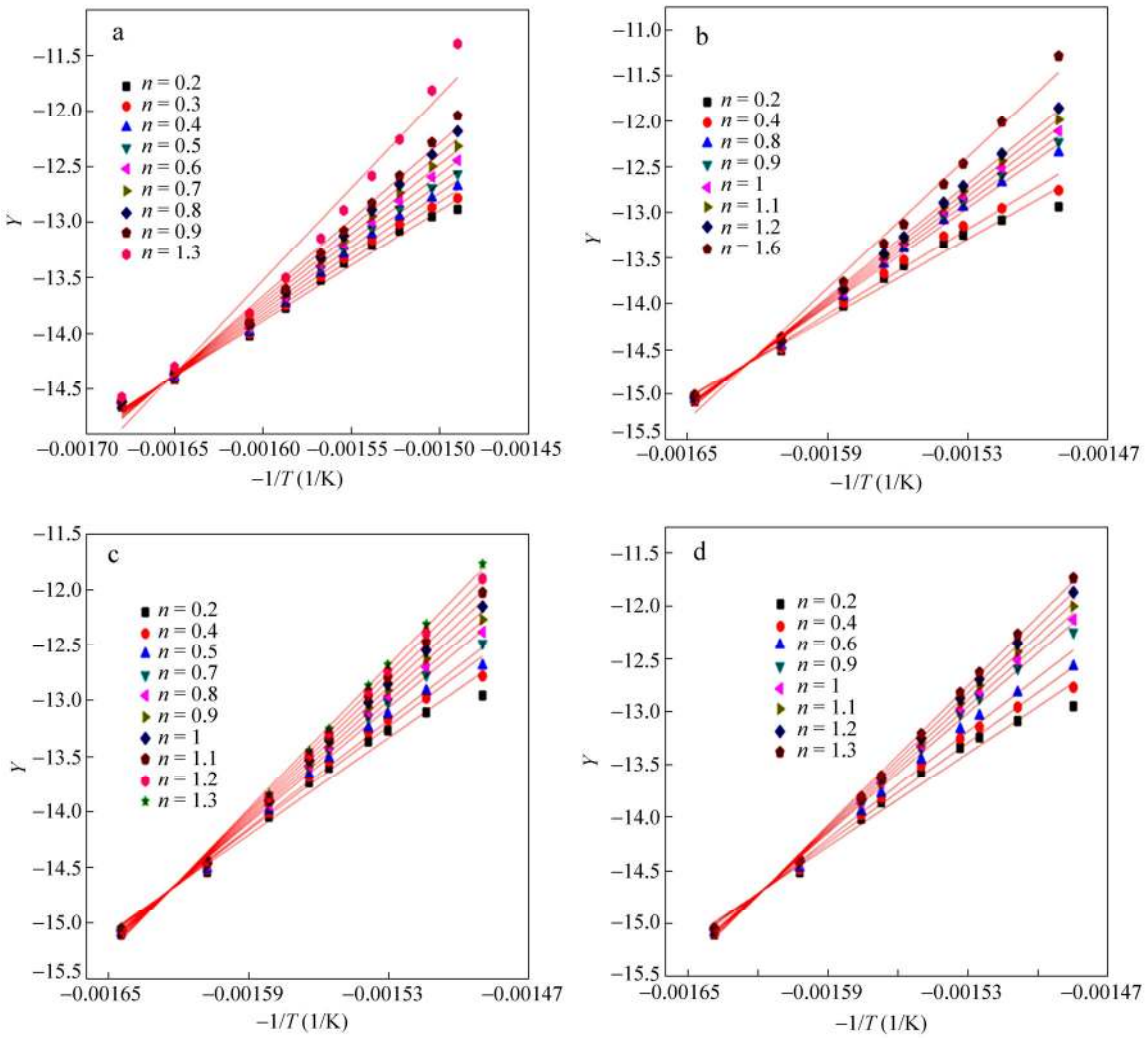

Fig. 8 Determination of kinetic parameters by plots of the left part in Eq. (1) against $-1/T$ using Coats-Redfern methods: (a) Pure PMMA, (b) PMMA/OLDH 3, (c) PMMA/OLDH 5 and (d) PMMA/OLDH 7 nanocomposites

Table 3 demonstrates that the activation energy (E_a) of PMMA/OLDH nanocomposites is 67–70 kJ/mol higher than that of pure PMMA. The PMMA/OLDH 7 is having the highest activation energy value among all other samples. Chen *et al.*[41] and Krishna and Pugazhenthi[42], also reported the improvement in activation energy of nanocomposites compared to neat polymer, which is in accordance with these findings.

Table 3. Kinetic parameters of different samples at the better correlation coefficient obtained from Coats-Redfern method at 10 K/min

Samples	E_a (kJ/mol)	A	n	R^2
Pure PMMA	99.4	3.862×10^7	0.6	0.996
PMMA/OLDH 3	167	1.190×10^{13}	1.1	0.998
PMMA/OLDH 5	167.1	1.243×10^{13}	1.1	0.998
PMMA/OLDH 7	170	1.942×10^{13}	1.1	0.998

Criado method

The kinetic parameters obtained from Coats-Redfern method are utilized to estimate the reaction mechanism of the system in Criado method[43] using the following expression.

$$Z(\alpha) = \frac{\beta}{A} g(\alpha) \frac{\mathrm{d}\alpha}{\mathrm{d}t} e^{\frac{E_a}{RT}} \tag{2a}$$

$$Z(\alpha) = \frac{\mathrm{d}\alpha}{\mathrm{d}t} \frac{E_a}{R} e^{\frac{E_a}{RT}} P(x) \tag{2b}$$

where $P(x)$ is determined using a biquadratic expression given by Senum *et al.*[44] and Flynn[45].

The kinetic parameters obtained from Coats-Redfern method are substituted into Eqs. (2a) and (2b). $Z(\alpha)$–α master curve is obtained by plotting Eq. (2a), using different reaction mechanism, $g(\alpha)$ given elsewhere[43]. The $Z(\alpha)$–α experimental curve is obtained by plotting $Z(\alpha)$ obtained from Eq. (2b) against α. Figures 9(a)–9(d) display the $Z(\alpha)$–α master and experimental curves for pure PMMA and PMMA nanocomposites with 3 wt%, 5 wt% and 7 wt% LDH loadings. It is apparent that for the pure PMMA, the experimental $Z(\alpha)$–α curve initially follows F1 reaction mechanism (random nucleation having one nucleus on individual particle) with lower α values ($\alpha < 0.4$) and then it deviates from F1 reaction mechanism to A4 mechanism (nucleation and growth) at higher α values ($\alpha = 0.8$–0.95). In the case of PMMA nanocomposites, the $Z(\alpha)$-α experimental curve follows the F1 reaction mechanism in the entire range of α.

Integral procedural decomposition temperature

The integral procedure decomposition temperature (IPDT) method was employed for the estimation of thermal stability of the nanocomposites as follows[46]:

$$\text{IPDT (°C)} = A \times K \times (T_f - T_i) + T_i \tag{3}$$

$$\text{where } A = (S_1 + S_2)/(S_1 + S_2 + S_3)$$

$$K = (S_1 + S_2)/(S_1)$$

where A is the area ratio of total experimental curve specified by the total TGA thermogram, T_i is the initial experimental temperature, T_f is the final experimental temperature. A graphical representation of a typical TGA thermogram divided into three areas of A_1, A_2, and A_3 is depicted in Fig. 10.

The IPDT values of all the samples are calculated using Eq. (3). In comparison with pure PMMA, the entire nanocomposites exhibit higher IPDT value indicating the increased thermal stability of the nanocomposites. The IPDT values of pure PMMA, PMMA nanocomposites with 3 wt%, 5 wt% and 7 wt% LDH loadings are 351.5, 399.4, 406.7 and 423.6 °C, respectively (see Table 2). The IPDT value of PMMA/OLDH 7 nanocomposite is the highest among other samples and similar result is also reflected in the TGA analysis. IPDT results are also consistent with activation energy calculation. A similar trend is also observed in our previous work on polystyrene/organoclay nanocomposites[42].

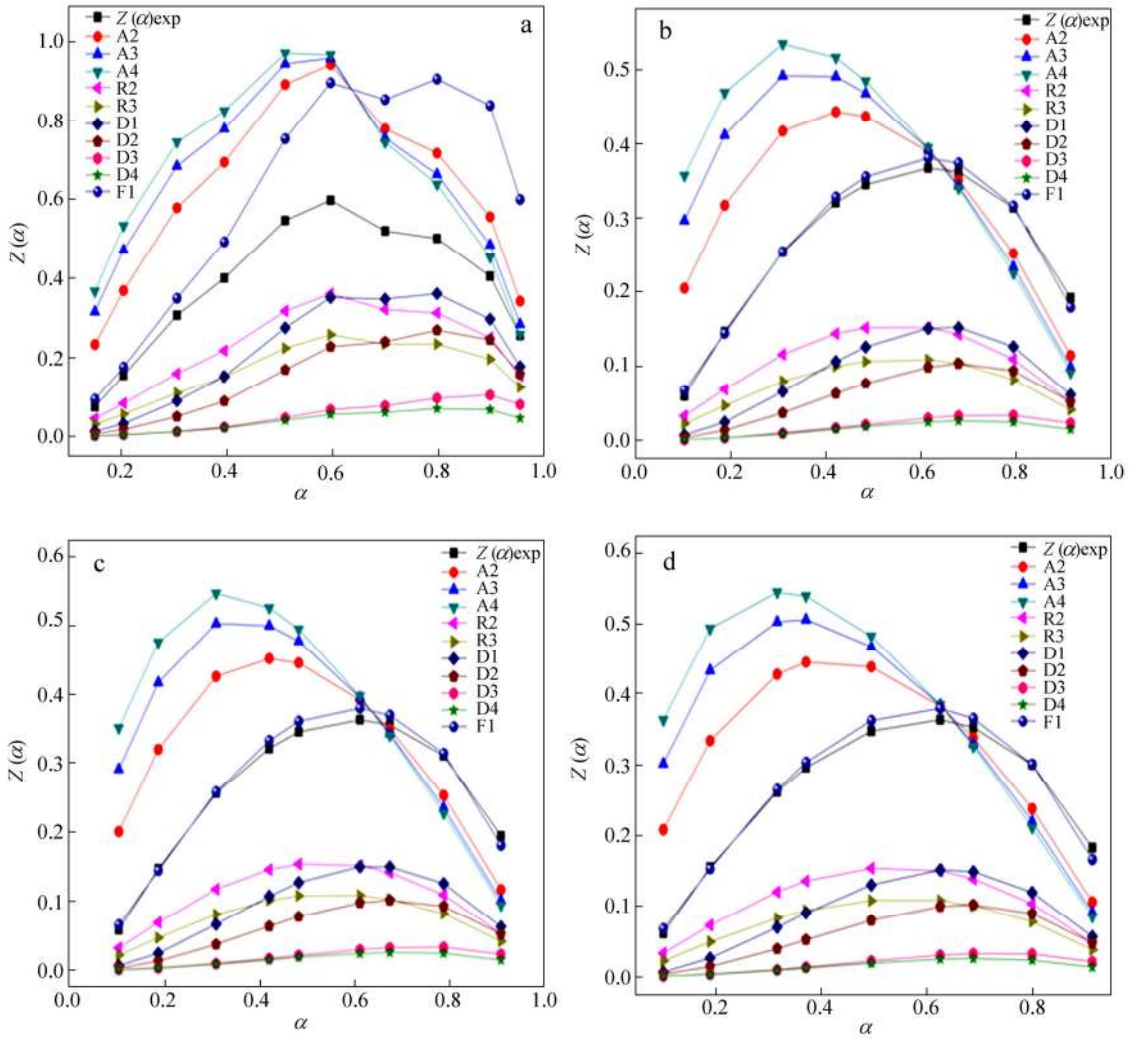

Fig. 9 Determination of thermal degradation mechanism by plotting $z(\alpha)$ versus α using Criado model: (a) pure PMMA, (b) PMMA/OLDH 3, (c) PMMA/OLDH 5 and (d) PMMA/OLDH 7 nanocomposites

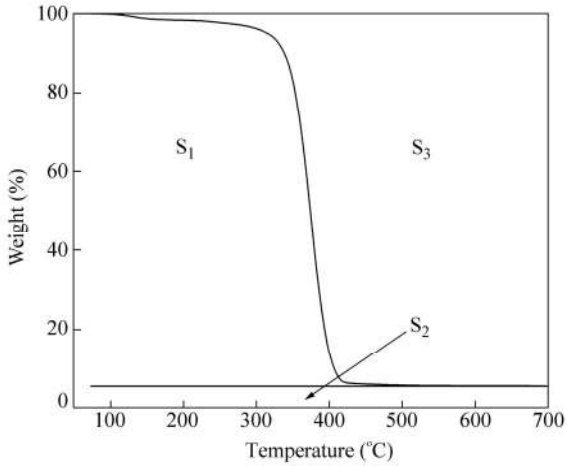

Fig. 10 Schematic for determining IPDT value of the nanocomposites

Water-uptake Test

The PMMA/OLDH nanocomposite films are tested for water uptake capacity. The result clearly signifies that, the water uptake capacity of PMMA nanocomposites decreases as the amount of LDH loading increases. The water uptake capacity of pure PMMA is 1.11%, while the water uptake capacities of PMMA/OLDH nanocomposite with 3 wt%, 5 wt% and 7 wt% LDH loadings are 0.86%, 0.82% and 0.63% respectively. The hydrophilic nature of LDH is reduced by the organic modification of LDH using SDS as modifier. Even though pure PMMA is hydrophobic in nature, the presence of modified LDH acts as an additional barrier against the water intake capacity of nanocomposites and making them more water resistant.

Rheological Analysis

Rheological analysis of polymer composites is a convenient method for inspecting the processing behavior and microstructure (distribution, concentration of filler and adhesion between polymer matrix and filler). Most of the polymer composites demonstrate a transition in rheological behavior from liquid to pseudo-solid or solid-like behavior with changing filler concentration. This transition is considered as the rheological percolation threshold. The frequency dependency of the storage modulus (G') and loss modulus (G''), is measured at 190 °C for the PMMA nanocomposites containing Ni-Al LDH and is depicted in Fig. 11. It is observed that Ni-Al LDH has an influential effect on the rheological behavior of polymer nanocomposites. As the LDH concentration increases, both storage modulus (G') and loss modulus (G'') increase, especially at lower frequencies.

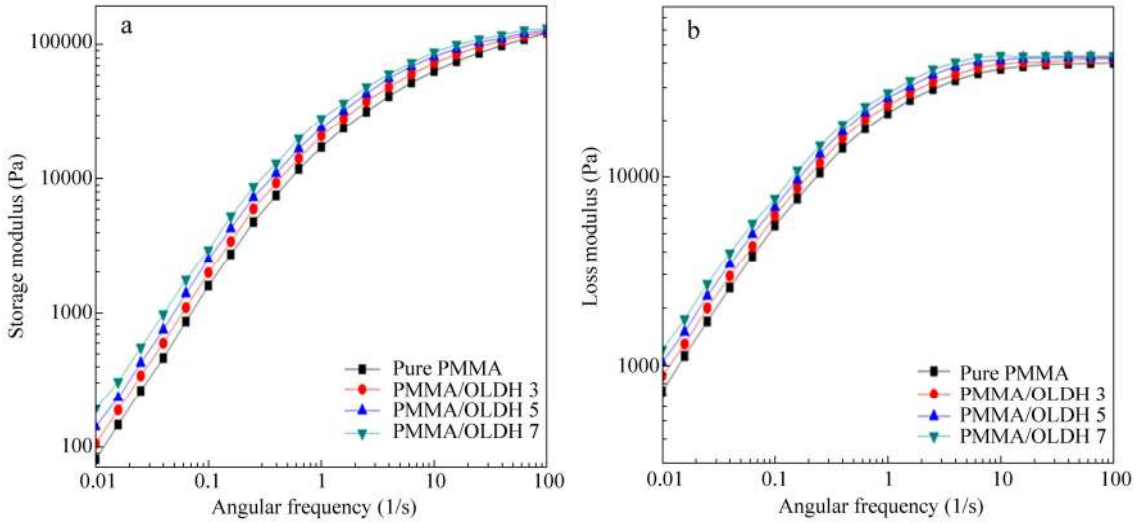

Fig. 11 (a) Storage modulus and (b) loss modulus of PMMA and its nanocomposites

The storage modulus G' gives a measure of 'elastic property' and its frequency dependency determines whether the material is in a liquid state or a solid state. The loss modulus G'' represents the 'viscous' characteristics of the given material. At 190 °C and low frequency, PMMA chains are fully relaxed and exhibit a typical homopolymer-like terminal behavior with the scaling properties of approximately $G' \sim \omega^2$ and $G'' \sim \omega$. As the frequency increases, the storage modulus is also enhanced with an increase in shear rate. This entire phenomenon indicates the behavior from a liquid-like to a solid-like viscoelastic, *i.e.* rheological percolation threshold and the formation of Ni-Al LDH-polymer chain networks, which restrain the long-range order of PMMA macromolecular chains. It is found from the loss modulus graph (Fig. 11b) that at lower frequencies, PMMA nanocomposites exhibit higher loss modulus when compared to pure PMMA. This suggests that LDH has pronounced effect on it. At higher shear rates, it is noticed that the long-time relaxation for all the compositions has perturbed and LDH has less effect. Similar findings are also noticed by Zhang *et al.*[47] for graphene based PMMA composites.

Complex viscosity is the frequency dependent viscosity determined during oscillation of shear stress. At lower frequencies or shear rates, the macromolecular chains are able to move slowly, glide along each other, and no energy is stored. Therefore, the range, where viscosity is constant, is considered as the zero-shear viscosity zone. It is also known as the terminal relaxation zone. The complex viscosity of PMMA and its nanocomposites analyzed at 190 °C is displayed in Fig. 12(a). As discussed earlier, the complex viscosity is higher at lower shear rates, due to terminal relaxation zone. As the frequency increases, the chains begin to orient in the flow direction and disentangle from one another and hence, the viscosity reduces. This suggests that viscosity is reduced due to partial disruption of three-dimensional network structures under oscillation at high frequencies.

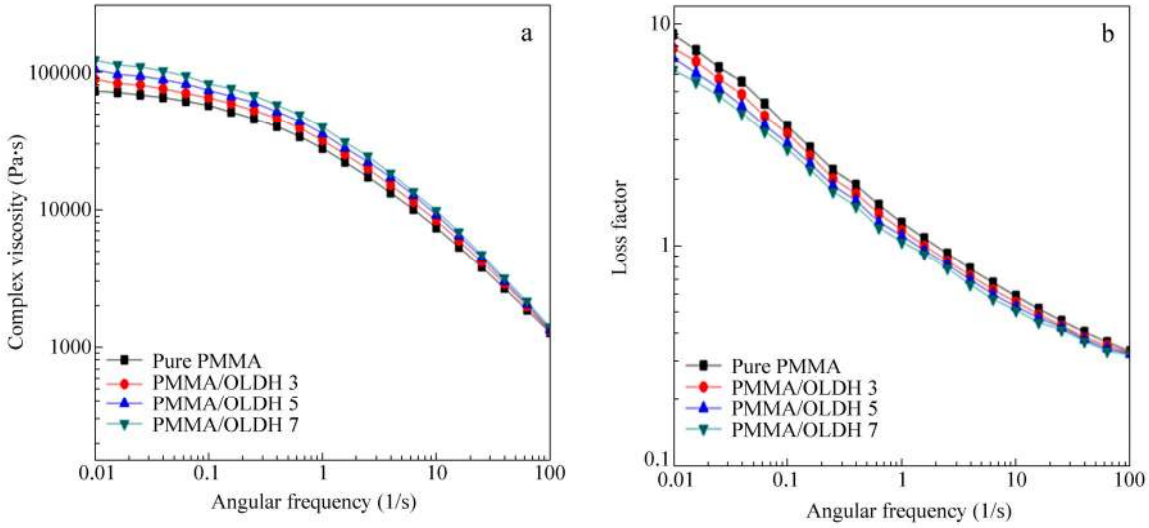

Fig. 12 (a) Complex viscosity and (b) damping factor of PMMA and its nanocomposites

The loss factor arises from the discordance between the strain and stress in the polymer nanocomposites exposed to an external force, which is strongly related to the applied frequency. The loss factor (tanδ) of PMMA and its nanocomposites is illustrated in Fig. 12(b). The loss factor is known as the ratio of loss modulus to storage modulus. The plot suggests that at lower frequencies, the loss factor is higher and a major drop is observed at the higher frequency region. At lower frequencies, the loss factor is higher due to the physical entanglements between the macromolecular chains and Ni-Al LDH, which cause the formation of some network structures. The decrease of loss factor in the higher frequency region is related to the partial orientation of polymer chains and LDH's as a result of shear deformation. Majid *et al.*[48] also reported similar type of reduction in loss factor for PP/ZnO nanocomposites.

CONCLUSIONS

PMMA/OLDH nanocomposites were prepared using solvent blending method. The influence of LDH loading on structural and thermal properties of PMMA/OLDH nanocomposites has been investigated. XRD and TEM analysis were done to define the structure of nanocomposite films. XRD analysis showed no diffraction peak (003), which clearly indicated the formation of exfoliated nanocomposites. TEM analyses were carried out to complement XRD results and displayed the formation of partially exfoliated nanocomposite structure. FTIR analysis confirms that the characteristics of both PMMA and modified Ni-Al LDH present in the nanocomposite samples. When 15% weight loss is taken as a point of comparison, the thermal decomposition temperature of PMMA/OLDH nanocomposites is 25–28 K higher than that of pure PMMA. The DSC clearly reveals that T_g of PMMA nanocomposites is marginally improved by 2 K to 3 K when compared to pure PMMA.

The activation energy and IPDT value of the PMMA nanocomposites enhance with increasing LDH loading

that clearly demonstrates the improved thermal stability of PMMA nanocomposites. The thermal degradation mechanism for pure PMMA follows the F1 mechanism at the initial stage of degradation and then it deviates from F1 reaction mechanism to A4 mechanism at higher α values. In case of PMMA nanocomposites, all the samples follow the F1 reaction mechanism in the entire range of α. Water intake capacity of PMMA nanocomposite samples decreases with increasing LDH loading. The storage and loss modulus increase as the frequency increases, and complex viscosity decreases with an increase in the frequency.

REFERENCES

1 Alexandre, M. and Dubois, P., Mater. Sci. Eng., R-Rep., 2000, 28: 1
2 Usuki, A., Kojima, Y., Kawasumi, M., Okada, A., Fukushima, Y., Kurauchi, T. and Kamigaito, O., J. Mater. Res., 1993, 8: 1179
3 Lan, T. and Pinnavaia, T.J., Chem. Mater., 1994, 6: 2216
4 Giannelis, E.P., Adv. Mater., 1996, 8: 29
5 Messersmith, P.B. and Giannelis, E.P., Chem. Mater., 1994, 6: 1719
6 Kojima, Y., Fukumori, K., Usuki, A., Okada, A. and Kurauchi, T., J. Mater. Sci. Lett., 1993, 12: 889
7 Wang, L., Xie, X., Su, S., Feng, J. and Wilkie, C.A., Polym. Degrad. Stab., 2010, 95: 572
8 Chen, W. and Qu, B., Chem. Mater., 2003, 15: 3208
9 Paul, D. and Robeson, L., Polymer, 2008 49: 3187
10 Wang, D.Y., Das, A., Leuteritz, A., Boldt, R., Häußler, L., Wagenknecht, U. and Heinrich, G., Polym. Degrad. Stab., 2011, 96: 285
11 Du, L., Qu, B. and Zhang, M., Polym. Degrad. Stab., 2007, 92: 497
12 Qiu, L., Chen, W. and Qu, B., Colloid. Polym. Sci., 2005, 283: 1241
13 Wang, G.A., Wang, C.C. and Chen, C.Y., Polym. Degrad. Stab., 2006, 91: 2443
14 Qiu, L. and Qu, B., J. Colloid Interface Sci., 2006, 301: 347
15 Huskić, M. and Žigon, M., Eur. Polym. J., 2007, 43: 4891
16 Krishna, S.V. and Pugazhenthi, G., J. Exp. Nanosci., 2012, 8: 19
17 Sahu, B. and Pugazhenthi, G., J. Appl. Polym. Sci., 2011, 120: 2485
18 Strawhecker, K.E. and Manias, E., Chem. Mater., 2000, 12: 2943
19 Unnikrishnan, L., Mohanty, S., Nayak, S.K. and Ali, A., Mater. Sci. Eng., A, 2011, 528: 3943
20 Leroux, F. and Besse, J.P., Chem. Mater., 2001, 13: 3507
21 Nalawade, P., Aware, B., Kadam, V. and Hirlekar, R., J. Sci. Ind. Res., 2009, 68: 267
22 Hong, N., Song, L., Wang, B., Stec., A.A., Hull, T.R., Zhan, J. and Hu, Y., Mater. Res. Bull., 2014, 49: 657
23 Li., M., Zhu, J.E., Zhang, L., Chen, X., Zhang, H., Zhang, F., Xu, S. and Evans, D.G., Nanoscale, 2011, 3: 4240
24 Wimalasiri, Y., Fan, R., Zhao, X.S. and Zou, L., Electrochim. Acta, 2014, 134: 127
25 Zhu, H., Liu, Q., Li, Z., Liu, J., Jing, X., Zhang, H. and Wang, J., RSC Adv., 2015, 5: 49204
26 Nyambo, C., Chen, D., Su, S. and Wilkie, C.A., Polym. Degrad. Stab., 2009, 94: 1298
27 Manzi-Nshuti, C., Wang, D., Hossenlopp, J.M. and Wilkie, C.A., Polym. Degrad. Stab., 2009, 94: 705
28 Li, B., Hu, Y., Liu, J., Chen, Z. and Fan, W., Colloid. Polym. Sci., 2003, 281: 998
29 Chen, W. and Qu, B., Polym. Degrad. Stab., 2005, 90: 162
30 Zhou, Z., Wang, S., Lu, L., Zhang, Y. and Zhang, Y., Compos. Sci. Technol., 2007, 67: 1861
31 Ivanov, I., Muke, S., Kao, N. and Bhattacharya, S.N., Polymer, 2001, 42: 9809
32 Al-Saleh, M.H. and Sundararaj, U., Composites Part A, 2011, 42: 2126
33 Ding, P. and Qu, B., J. Colloid Interface Sci., 2005, 291: 13
34 Gilman, J.W., Jackson, C.L., Morgan, A.B., Harris, Jr. R., Manias, E., Giannelis, E. P., Wuthenow, M., Hilton, D. and Philips, S.H., Chem. Mater., 2002, 12: 1886
35 Tomar, A., Mahendia, S. and Kumar, S., Adv. Appl. Sci. Res., 2011, 2: 65

36 Morgan, A.B. and Gilman, J.W., J. Appl. Polym. Sci., 2003, 87: 1329
37 Mohanty, S. and Nayak, S.K., J. Thermoplast. Compos., 2010, 23: 623
38 Shen, Z., Simon, G.P. and Cheng, Y.B., J. Appl. Polym. Sci., 2004, 92: 2101
39 Stretz, H.A., Paul, D.R., Li, R., Keskkula, H. and Cassidy, P.E., Polymer, 2005, 46: 2621
40 Coats, A.W. and Redfern, J.P., Nature, 1964, 201: 68
41 Chen, Y. and Wang, Q., Polym. Degrad. Stab., 2007, 92: 280
42 Krishna, S. and Pugazhenthi, G., J. Appl. Polym. Sci., 2011, 120: 1322
43 Criado, J.M., Málek, J. and Ortega, A., Thermochim. Acta, 1989, 147: 377
44 Senum, G.I. and Yang, R.T., J. Therm. Anal., 1977, 11: 445
45 Flynn, J.H., Thermochim. Acta, 1997, 300: 83
46 Park, S.J., Li, K. and Hong, S.K., J. Ind. Eng. Chem., 2005, 11: 561
47 Zhang, H.B., Zheng, W.G., Yan, Q., Jiang, Z.G. and Yu, Z.Z., Carbon, 2012, 50: 5117
48 Majid, M., Hassan, E.D., Davoud, A. and Saman, M., Composites Part B, 2011, 42: 2038